


## Hydrogen sulfide attenuates diabetic neuropathic pain through NO/cGMP/PKG pathway and $\mu$ -opioid receptor

Hao Li<sup>1,\*</sup>, Shulin Liu<sup>2,\*</sup>, Zheng Wang<sup>3</sup>, Yonglai Zhang<sup>4</sup> and Kaiguo Wang<sup>4</sup> 

<sup>1</sup>Medical Management Department, Shandong Cancer Hospital and Institute, Shandong First Medical University and Shandong Academy of Medical Sciences, Shandong 250117, China; <sup>2</sup>Department of Aviation Medicine, Naval Medical Institute, Second Military Medical University, Shanghai 200433, China; <sup>3</sup>Pre Hospital Emergency Department, Shandong Otolaryngology Hospital Affiliated to Shandong University (West Hospital of Shandong Provincial Hospital), Shandong 250117, China; <sup>4</sup>Department of Anesthesiology, Shandong Cancer Hospital and Institute, Shandong First Medical University and Shandong Academy of Medical Sciences, Shandong 250117, China

Corresponding author: Kaiguo Wang. Email: kaiguosd@sina.com

\*These authors contributed equally to this study.

### Impact statement

There are currently approximately 425 million diabetic patients worldwide, of which approximately 90% of patients with diabetes suffer from neuropathy. Diabetic neuropathic pain (DNP) is a common complication of diabetic neuropathy. Nearly half of the patients hospitalized with diabetes have pain symptoms or symptoms related to neurological injury, and the incidence increases with age and diabetic duration. Anti-DNP analgesics have either limited therapeutic effects or serious side effects or lack of clinical trials, which has limited their application.

Physiopathological mechanisms and treatment of DNP remain a significant challenge. The present confirmed that inhalation of H<sub>2</sub>S may attenuate the diabetic neuropathic pain through NO/cGMP/PKG pathway and  $\mu$ -opioid receptor. It provides us the animal study foundation for the application of H<sub>2</sub>S on the treatment of DNP and clarifies some target molecules in the pain modulation of DNP.

### Abstract

Diabetic neuropathic pain is a frequent complication of diabetic neuropathy. The specific manifestations of diabetic neuropathic pain include spontaneous pain and hyperalgesia, which seriously affect the quality of life of patients. Previous publications have shown that H<sub>2</sub>S has both pro-nociceptive and anti-nociceptive effects. This present investigation aimed to examine the anti-nociceptive effect of H<sub>2</sub>S on diabetic neuropathic pain. We established a diabetic neuropathic pain animal model with high-glucose, high-fat diet, and STZ, then treated rats with different concentrations of H<sub>2</sub>S and inhibitors of NOS, sGC, PKG, and opioid receptors. The mechanical allodynia and thermal hyperalgesia of rats were measured to assess the anti-nociceptive effects of H<sub>2</sub>S. The mRNA and protein expression of NOS and PKG1 were measured to explore their roles in the anti-nociceptive action of H<sub>2</sub>S. The results revealed that inhalation of H<sub>2</sub>S gas had anti-nociceptive effect in diabetic neuropathic pain model rats without affecting the blood glucose level and body mass. It increased the mRNA and protein level of nNOS, and the inhibitor of nNOS, 7-NI, abolished the anti-nociceptive effect of H<sub>2</sub>S. Furthermore, inhibitors of sGC and PKG could also abolish the anti-nociceptive effect of H<sub>2</sub>S. The expression of PKG1 was found to be increased by H<sub>2</sub>S, which was reversed by the inhibitors of nNOS, sGC, and PKG. Finally, CTOP, a  $\mu$ -opioid receptor antagonist, abolished the anti-nociceptive effect of H<sub>2</sub>S, indicating that the  $\mu$ -opioid receptor plays a role in the anti-nociceptive effect of H<sub>2</sub>S. In conclusion, the findings of this investigation suggest that hydrogen sulfide may attenuate the diabetic neuropathic pain through NO/cGMP/PKG pathway and  $\mu$ -opioid receptor.

**Keywords:** Hydrogen sulfide, diabetic neuropathic pain, nitric oxide, cGMP, PKG,  $\mu$ -opioid receptor

**Experimental Biology and Medicine 2020; 245: 823–834. DOI: 10.1177/1535370220918193**

### Introduction

In recent years, as a result of high-sugar and high-fat diet habits, the incidence of diabetes and its complications has increased dramatically.<sup>1</sup> The main complications of diabetes include kidney disease, cardio-cerebral vascular

disease, retinopathy, nerve damage, etc. There are currently approximately 425 million diabetic patients worldwide, of which approximately between 6% and 51% among adults with diabetes suffer from neuropathy.<sup>2</sup> Neuropathic pain is triggered by the primary injury of the nervous system.

The main manifestations include spontaneous pain, hyperalgesia, abnormal pain, and paresthesia.<sup>3</sup> Diabetic neuropathic pain (DNP) is a frequent complication of diabetes. Nearly half of the patients hospitalized with diabetes have pain symptoms or symptoms related to neurological injury, and the incidence increases with age and diabetic duration.<sup>4</sup> The pathogenesis is not clear yet. It is speculated that it may be related to the combined effects of metabolic disorders, reduced neurotrophic factors, and autoimmune factors caused by hyperglycemia.<sup>5,6</sup> The high glucose state during diabetes can cause a large number of body peroxides, which causes oxidative stress and promotes the release of pro-inflammatory factors. These actions aggravate nervous system damage and promote the progress of DNP.<sup>7</sup> The specific manifestations of DNP include spontaneous pain and hyperalgesia, which seriously affect the quality of life of patients.<sup>2</sup> Although there have been some publications on the pathogenesis of DNP, including the involvement of  $\mu$ -opioid receptor,<sup>8</sup> there are many factors involved in the formation and maintenance of DNP, and multiple mechanisms are involved.<sup>8-11</sup> Anti-DNP analgesics have either limited therapeutic effects or serious side effects or lack of clinical trials,<sup>12</sup> which has limited their application.

To explore the new treatment of DNP, hydrogen sulfide ( $H_2S$ ) may be a potential candidate. As a new type of gas molecule,  $H_2S$  plays an important role in many physiological functions.<sup>13</sup> It is involved in many diseases.<sup>14</sup> Endogenous  $H_2S$  can be produced by the catalyzation of L-cysteine by cystathionine  $\beta$ -synthase.<sup>15</sup> In recent years, much literature has shown that  $H_2S$  is involved in the modulation of pain processing as a neuromodulator.<sup>16-19</sup> It has been shown that  $H_2S$  has both pro-nociceptive and anti-nociceptive effects. Previous studies showed that the local administration of  $H_2S$  had a nociception effect. Injection of  $H_2S$  donor sodium sulfide into the foot can induce hyperalgesia, which can be blocked by oxidants.<sup>16</sup> The ipsilateral hindfoot hyperalgesia induced by the injection of formalin is related to the increase in the concentration of  $H_2S$  at the injection site, without causing the contralateral hindfoot hyperalgesia.<sup>17</sup> However, there are also reports that the systemic administration of  $H_2S$  can produce an anti-nociceptive effect. For example, the treatment of NaHS suppresses nociception induced by colorectal distension, which is regulated by K(ATP) channels and nitric oxide (NO).<sup>20</sup> Chen *et al.*<sup>21</sup> found that NaHS exhibited an anti-nociceptive effect in neuropathic pain established by chronic constriction injury. It was also revealed that  $H_2S$  prevents bone cancer pain.<sup>22</sup>

$H_2S$  exerts its biological characteristics through ATP-sensitive potassium channels, transient receptor potential-A channels, and nitric oxide synthase (NOS).<sup>23-25</sup> It is reported that NO and cGMP can activate downstream molecules, including cGMP-dependent protein kinase (PKG) and potassium channels.<sup>26,27</sup> The NO/cGMP/PKG signaling participates in diabetes-associated osteoporosis.<sup>28</sup> Besides, in the analgesic effects produced by clonidine ( $\alpha$ 2 adrenergic receptor agonist), neostigmine (cholinesterase inhibitor), and [D-Pen2,D-Pen5]-enkephalin ( $\delta$ -opioid

receptor agonist), NO plays an important role.<sup>29</sup> When S-Nitroso-N-acetylpenicillamine (NO donor) is used in combination with L-cysteine, it produces anti-nociceptive effect.<sup>30</sup> There are also reports that stimulation of the NO/cGMP/PKG signal leads to the opening of ATP-dependent potassium channels and the production of anti-nociceptive effect.<sup>31</sup>

Although  $H_2S$  shows a great possibility to exert an anti-nociceptive effect, the effect of  $H_2S$  on DNP has not been reported yet. Therefore, this work was performed to examine the anti-nociceptive effect of  $H_2S$  on DNP. The involvement of NO/cGMP/PKG signaling pathway and  $\mu$ -opioid receptor was investigated to explore the mechanism. The hypothesis is  $H_2S$  may exert an anti-nociceptive effect on DNP through a NO/cGMP/PKG signaling pathway and  $\mu$ -opioid receptor.

## Materials and methods

### Animals and treatment

A total of 650 male Sprague-Dawley rats (180–220 g, aging 6–7 weeks) were provided by the Shandong Cancer Hospital animal center and kept there. All rats were housed under 23–25°C and 65–75% humidity with free access to food and water. The procedures of this investigation complied with IASP's ethical guidelines. Approval by the Animal Care and Use Committee of Shandong First Medical University has been obtained.

Rats were treated with four weeks of a high-glucose, high-fat diet, 12 h of starvation, and a single peritoneal injection (i.p.) of Streptozocin (STZ, 35 mg/kg). One week later, we began to measure the blood glucose level, body mass and mechanical allodynia (MA), and thermal hyperalgesia (TH) (once a week). At the second week point, rats who meet the criteria for diabetic neuropathic pain (DNP) according to the blood glucose level and MA/TH were assigned to groups. If the blood glucose exceeded 300.6 mg/dL, and the MA/TH were different from Control, the DNP model was considered to be successfully established. Animals were then randomly assigned to groups ( $n = 12$ ). Excess rats were sacrificed.

In experiment 1, 70 rats were used to induce DNP model, and 56 rats were considered to meet DNP criteria. These rats and 24 normal rats were randomly assigned into Control, DNP model, DNP model +  $H_2S$ -L, DNP model +  $H_2S$ -M, DNP model +  $H_2S$ -H, and  $H_2S$ -M groups. Rats in the Control group received no treatment (feed with normal diet); Rats in the DNP model group received DNP model treatment; Rats in the DNP model +  $H_2S$ -L, DNP model +  $H_2S$ -M, DNP model +  $H_2S$ -H groups received DNP model treatment and inhaled different concentrations of  $H_2S$ . Rats in the  $H_2S$ -M group only inhaled 20 ppm  $H_2S$  (feed with normal diet). The  $H_2S$  inhalation started at two weeks post-STZ injection for 2 h per day.

In experiment 2, 150 rats were used to induce the DNP model; 130 rats were considered to meet the DNP criteria. Rats were randomly assigned into Vehicle,  $H_2S$ -M,  $H_2S$ -M + 1400W-L,  $H_2S$ -M + 1400W-M,  $H_2S$ -M + 1400W-H,  $H_2S$ -M + 7-NI-L,  $H_2S$ -M + 7-NI-M,  $H_2S$ -M + 7-NI-H

groups. In experiment 3, 150 rats were used to induce the DNP model; 132 rats were considered to meet DNP criteria. Rats were randomly assigned into Vehicle, H2S-M, H2S-M + ODQ-L, H2S-M + ODQ-M, H2S-M + ODQ-H, H2S-M + KT5823-L, H2S-M + KT5823-M, H2S-M + KT5823-H groups. In experiment 4, 250 rats were used to induce the DNP model; 192 rats were considered to meet the DNP criteria. Rats were randomly assigned into Vehicle, H2S-M, H2S-M + Nor-BNI-L, H2S-M + Nor-BNI-M, H2S-M + Nor-BNI-H, H2S-M + CTOP-L, H2S-M + CTOP-M, H2S-M + CTOP-H groups, H2S-M + Naltrindole-L, H2S-M + Naltrindole-M, H2S-M + Naltrindole-H. All rats received DNP model treatment. Rats in the Vehicle group were given saline via intrathecal polyethylene catheter. Rats in the H2S-M group inhaled 20 ppm H2S. Rats in H2S-M + 1400W groups, H2S-M + 7-NI groups, H2S-M + ODQ groups, H2S-M + KT5823 groups, H2S-M + Nor-BNI groups, H2S-M + CTOP groups, and H2S-M + Naltrindole groups inhaled 20 ppm H2S and were given different concentrations of 1400 W, 7-NI, ODQ, KT5823, Nor-BNI, CTOP, or naltrindole via intrathecal polyethylene catheter. The intrathecal injection of drugs started at two weeks post-STZ injection and lasted for a week.

### Establishment of DNP animal model

The preparation procedure of the DNP animal model was similar to the literature of Ge *et al.*<sup>32</sup> The model was induced by four weeks of a high-glucose, high-fat diet, 12 h of starvation, and an injection (i.p.) of streptozocin (STZ, 35 mg/kg). Blood was collected after food consumption and the blood glucose was measured every week. If it exceeded 300.6 mg/dL, rats were considered as "type 2 diabetes mellitus." The body mass was also measured every week. The mechanical withdrawal threshold (MWT) and thermal withdrawal latency (TWL) were examined every Monday for six weeks, beginning from one-week post-STZ injection. If the rats had evident MA/TH, the DNP model was considered as successfully established.<sup>33</sup>

### H<sub>2</sub>S inhalation

The H<sub>2</sub>S inhalation procedure has been described by Kida *et al.*<sup>34</sup> Briefly, beginning at two weeks post-STZ injection, rats inhaled H<sub>2</sub>S for 2 h each day. The H<sub>2</sub>S inhalation was completed using a 28-L transparent plastic chamber (Ningbo Chamber Company, Ningbo, China). Rats were put in the chamber to the air-H<sub>2</sub>S mixture for 2 h per day at room pressure. The H<sub>2</sub>S concentration was kept at 10 ppm (H<sub>2</sub>S-L), 20 ppm (H<sub>2</sub>S-M), or 40 ppm (H<sub>2</sub>S-H). The H<sub>2</sub>S concentration was monitored with an ONIX CVI H<sub>2</sub>S analyzer.<sup>35</sup>

### Intrathecal injection of inhibitors

The inhibitors of iNOS (1400 W), nNOS (7-NI), soluble guanylate cyclase (sGC) (ODQ), PKG (KT5823), and antagonists of  $\kappa$ -opioid receptor antagonist (Nor-BNI),  $\mu$ -opioid receptor (CTOP), and  $\delta$ -opioid receptor (naltrindole) were administered by intrathecal injection at the first week after STZ injection. ODQ was used to inhibit sGC, so the produce

of cGMP was decreased. The procedure has been described by Chen *et al.*<sup>36</sup> Firstly, rats were anesthetized with ketamine (100 mg/kg, i.m.) and xylazine (7.5 mg/kg, i.m.). An incision was made in the gap between the L4/L5 vertebrae to insert a polyethylene catheter (PE-10, Instech Laboratories, PA, USA) so its tip was positioned at the sub-arachnoid space. The catheter was connected to a dorsally subcutaneously implanted Alzets osmotic minipump (1007D) with polyvinylchloride tubing, as reported in our previous study.<sup>37</sup> It has a 100- $\mu$ L reservoir and delivers drug at a rate of 0.5  $\mu$ L/h for a week. Every compound was given at three concentrations; 1400 W was given at 1  $\mu$ g/10  $\mu$ L (1400 W-L), 5  $\mu$ g/10  $\mu$ L (1400 W-M), 10  $\mu$ g/10  $\mu$ L (1400 W-H); 7-NI was given at 1  $\mu$ g/10  $\mu$ L (7-NI-L), 10  $\mu$ g/10  $\mu$ L (7-NI-M), 100  $\mu$ g/10  $\mu$ L (7-NI-H); ODQ was given at 1  $\mu$ g/10  $\mu$ L (ODQ-L), 10  $\mu$ g/10  $\mu$ L (ODQ-M), 20  $\mu$ g/10  $\mu$ L (ODQ-H); KT5823 was given at 100 ng/10  $\mu$ L (KT5823-L), 500 ng/10  $\mu$ L (KT5823-M), 1  $\mu$ g/10  $\mu$ L (KT5823-H); Nor-BNI was given at 10  $\mu$ g/10  $\mu$ L (Nor-BNI-L), 20  $\mu$ g/10  $\mu$ L (Nor-BNI-M), 40  $\mu$ g/10  $\mu$ L (Nor-BNI-H); CTOP was given at 1  $\mu$ g/10  $\mu$ L (CTOP-L), 10  $\mu$ g/10  $\mu$ L (CTOP-M), 20  $\mu$ g/10  $\mu$ L (CTOP-H); Naltrindole was given at 5  $\mu$ g/10  $\mu$ L (Naltrindole-L), 10  $\mu$ g/10  $\mu$ L (Naltrindole-M), 20  $\mu$ g/10  $\mu$ L (Naltrindole-H). All these compounds were provided by Santa Cruz (CA, USA).

### Measurement of MWT and TWL

The Von Frey filament method was applied to measure the mechanical allodynia.<sup>37</sup> The measurement was carried out between 10:00 a.m. and 4:00 p.m., and the ambient temperature was maintained at 20–25°C. Rats were placed on a test rack made of metal in a Plexiglas box. Before the measurement, the rats had 15 min to adapt to the environment. The Von Frey filaments (0.6 g–1.5 g) are used in the study, which are gradually pressurized to bend the filaments when stimulating the paws of the rats. The continuing stimulation duration was 3 s and the measurement interval is 15 s. The minimum value of the Von-Fery filament (5 times) recorded when the paws of rat were lifted was regarded as the MWT.

The measurement of TWL was performed with a paw thermal stimulator in a quiet environment at room temperature. First, the distance of the thermal stimulator and the size of the light source were adjusted. After rats have fully adapted to the test environment for 20 min, the thermal stimulator was aimed at the left hind foot of rats. The light of the thermal stimulator was turned on and the timer started at the same time. When the rats lifted their feet, the timing stopped and the time was recorded as TWL. Three measurements were taken on each left hind foot of the rat at 10-min intervals. The maximum time of TWL measurement was set as 30 s to prevent the feet of the rats from being burned. If the rat has not escaped or lifted its feet after 30 s, the thermal stimulation would automatically stop and the TWL was recorded as 30 s.<sup>38</sup>

### Real-time PCR analysis

At the end of six weeks after STZ injection, rats were sacrificed by exsanguination under anesthesia after the

assessment of MA/TH was completed. The L4-L6 spinal cord was collected to measure the mRNA levels of iNOS, eNOS, nNOS, and PKG1 using real-time PCR method.<sup>39</sup> The primer sequences for iNOS, eNOS, nNOS, and PKG1 were as follows: iNOS, 5'-ACAGGGAAGTCTGAAGC ACTAG-3' (coding sense), 5'-CATGCAAGGAAGGAA CTCTTC-3' (coding antisense); eNOS, 5'-CTATGGTAGT GCCTTGGCTGGAGG-3' (coding sense), 5'-ACCGCCCA GGGAACTCCGCT-3' (coding antisense); nNOS, 5'-TA GCTTCCAGAGTGACAAAGTGACC-3' (coding sense), 5'-TGTTCCAGGGATCAGGCTGGTATTC-3' (coding antisense); PKG1, 5'-CCG AATTCTGTATTTCTTACCTGC TTC-3' (coding sense), 5'-CACACTAGTGGACTCAGTT TAATTTGTGG-3' (coding antisense);  $\beta$ -actin, 5'-CACC CGCGAGTACAACCTTC-3' (coding sense), 5'-CCCAT ACCCACCATCACACC-3' (coding antisense). The results were expressed as the ratio of Control.

### Western blot analysis

At the end of six weeks after STZ injection, rats were sacrificed by exsanguination under anesthesia after the assessment of MA/TH was completed. Samples for RT-PCR and Western Blot were collected from the same rats. The L4-L6 spinal cord of rats was collected to measure the protein levels of iNOS, eNOS, nNOS, and PKG1 using the Western Blot method.<sup>39</sup> Briefly, the L4-L6 spinal cord was first homogenized (1000 $\times$ g, 15 min) to collect the protein, which were separated by an SDS-PAGE gel and transferred to a nitrocellulose membrane, which was then incubated with primary antibodies of iNOS, eNOS, nNOS, PKG1, and  $\beta$ -actin overnight at 4°C, and with secondary antibody (1:2000; Santa Cruz, USA) at 25°C for 1 h. The primary antibodies were provided by Sigma-Aldrich (St. Louis, MO, USA). The protein expression level was measured using the Quantity One software (Bio-Rad, Hercules, USA).

### Statistical analysis

Data were presented as the Mean  $\pm$  S.E.M and analyzed by one-way ANOVA and Bonferroni post hoc test. For MWT, TWL, blood glucose, and body mass, the comparison was performed between data in the same week.  $P < 0.05$  was regarded statistically significant.

## Results

### H<sub>2</sub>S exerted antinociceptive effect in DNP model rats

Figure 1 shows the changes in MWT and TWL of rats. The MWT and TWL were dramatically decreased over-time in the DNP group. Treatment of lower concentration of H<sub>2</sub>S did not significantly change the MWT and TWL compared to Control, but treatment of middle and higher concentrations of H<sub>2</sub>S significantly increased them from the fourth week after STZ treatment compared to DNP group (MWT:  $P < 0.05$ ,  $F = 15.90$ ,  $df = 5$ ,  $R^2 = 0.5409$ ; DNP model + H<sub>2</sub>S-M vs. DNP model,  $P < 0.05$ , Mean Diff. = -9.354,  $t = 4.731$ ; DNP model + H<sub>2</sub>S-H vs. DNP model,  $P < 0.05$ , Mean Diff. = -9.934,  $t = 5.024$ . TWL:  $P < 0.05$ ,  $F = 8.702$ ,  $R^2 = 0.3919$ ; DNP model + H<sub>2</sub>S-M vs. DNP model,  $P < 0.05$ , Mean Diff. = 6.640,  $t = 4.072$ ; DNP model + H<sub>2</sub>S-H vs. DNP model,  $P < 0.05$ , Mean Diff. = 4.600,  $t = 2.821$ ). Treatment of middle concentration of H<sub>2</sub>S only (without STZ injection) did not impact the MWT and TWL of rats compared to Control.

### H<sub>2</sub>S did not impact the blood glucose level or body mass

The changes in blood glucose level and body mass of rats are shown in Figure 2. The blood glucose level of rats in the DNP model group was significantly increased ( $P < 0.05$ ,  $F = 78.94$ ,  $df = 5$ , Mean Diff. = 14.81,  $t = 0.6422$ ). Treatment of three concentrations of H<sub>2</sub>S did not significantly change the blood glucose level compared to the DNP model group ( $P > 0.05$ ). Treatment of the middle concentration of H<sub>2</sub>S

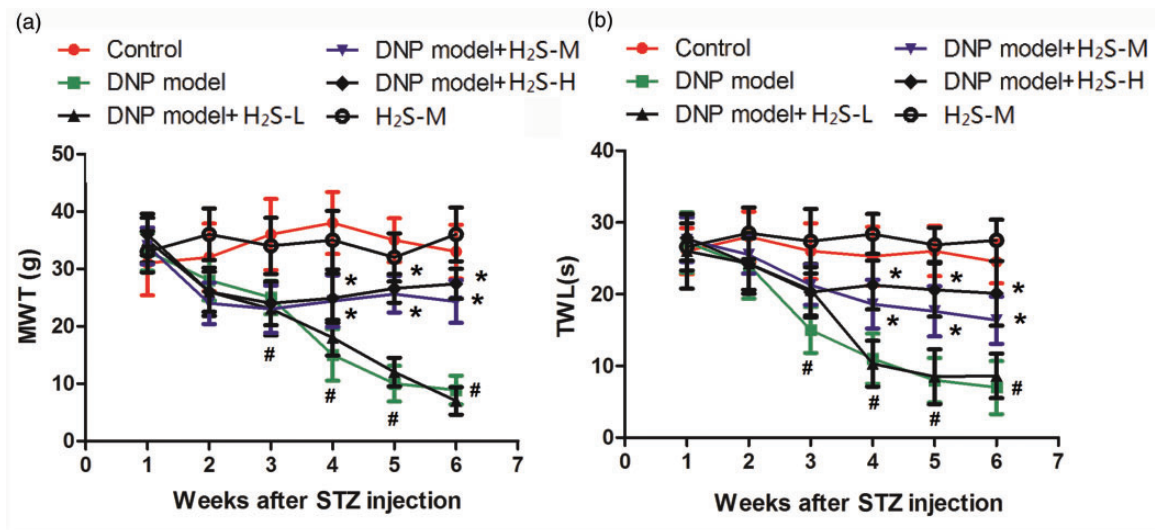


**Figure 1.** Changes in the mechanical allodynia and thermal hyperalgesia of rats. Figure 1 shows the changes in MWT and TWL of rats. The values are expressed as Mean  $\pm$  S.E.M. The MWT (a) and TWL (b) of rats were measured every Monday for six weeks, beginning from one-week post-STZ injection. H<sub>2</sub>S-L: lower concentration of H<sub>2</sub>S (10 ppm); H<sub>2</sub>S-M: middle concentration of H<sub>2</sub>S (20 ppm); H<sub>2</sub>S-H: higher concentration of H<sub>2</sub>S (40 ppm). MWT: mechanical withdrawal threshold; TWL: thermal withdrawal latency. # $P < 0.05$  compared to Control; \* $P < 0.05$  compared to DNP model.  $n = 12$  per group. (A color version of this figure is available in the online journal.)

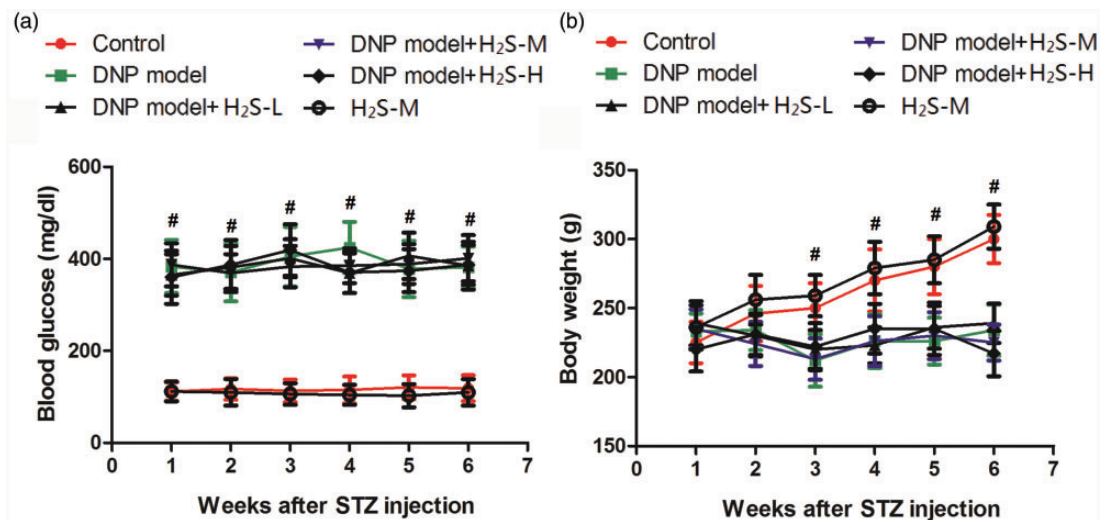


**Figure 2.** Changes in the blood glucose level and body mass of rats. Figure 2 shows the changes in blood glucose level and body mass of rats. The values are expressed as Mean  $\pm$  S.E.M. The blood glucose level (a) and body mass (b) were measured every Monday for six weeks, beginning from one-week post-STZ injection. H<sub>2</sub>S-L: lower concentration of H<sub>2</sub>S (10 ppm); H<sub>2</sub>S-M: middle concentration of H<sub>2</sub>S (20 ppm); H<sub>2</sub>S-H: higher concentration of H<sub>2</sub>S (40 ppm). #*P* < 0.05 compared to Control. *n* = 12 per group. (A color version of this figure is available in the online journal.)

only did not impact the blood glucose level ( $P > 0.05$ ). As shown in Figure 2(b), the body mass of rats in the Control group and H<sub>2</sub>S-M group gradually increased over-time, but the body mass of rats in the DNP model group, DNP model + H<sub>2</sub>S-L, DNP model + H<sub>2</sub>S-M, and DNP model + H<sub>2</sub>S-H groups did not show an increase over-time. From the third week post-STZ injection, the body mass of rats in the DNP model group, DNP model + H<sub>2</sub>S-L, DNP model + H<sub>2</sub>S-M, and DNP model + H<sub>2</sub>S-H groups was significantly lower than Control ( $P < 0.05$ ,  $F = 9.467$ ,  $df = 5$ ,  $R^2 = 0.4570$ ; DNP model vs. Control,  $P < 0.05$ , Mean Diff. =  $-41.10$ ,  $t = 5.482$ ; DNP model + H<sub>2</sub>S-L vs. Control,  $P < 0.05$ , Mean Diff. =  $30.90$ ,  $t = 4.122$ ; DNP model + H<sub>2</sub>S-M vs. Control,  $P < 0.05$ , Mean Diff. =  $-38.00$ ,  $t = 5.069$ ; DNP model + H<sub>2</sub>S-H vs. Control,  $P < 0.05$ , Mean Diff. =  $-28.70$ ,  $t = 3.828$ ). No significant difference was observed in the body mass between the DNP model group and DNP model + H<sub>2</sub>S-L, DNP model + H<sub>2</sub>S-M, or DNP model + H<sub>2</sub>S-H groups ( $P > 0.05$ ). It is indicated that H<sub>2</sub>S did not impact the blood glucose level or the body mass.

### H<sub>2</sub>S increased the mRNA and protein level of nNOS, but not iNOS or eNOS

The mRNA level of iNOS, eNOS, and nNOS and their protein expression level were measured with the Western blot method. As shown in Figure 3, the mRNA and protein level of iNOS were enhanced in the DNP groups (mRNA:  $P < 0.05$ ,  $F = 182.7$ ,  $df = 5$ ,  $R^2 = 0.9420$ ; DNP model vs. Control,  $P < 0.05$ , Mean Diff. =  $3.747$ ,  $t = 22.72$ ; DNP model + H<sub>2</sub>S-L vs. Control,  $P < 0.05$ , Mean Diff. =  $-3.587$ ,  $t = 21.75$ ; DNP model + H<sub>2</sub>S-M vs. Control,  $P < 0.05$ , Mean Diff. =  $3.427$ ,  $t = 20.78$ ; DNP model + H<sub>2</sub>S-H vs. Control,  $P < 0.05$ , Mean Diff. =  $3.237$ ,  $t = 19.62$ . Protein level:  $P < 0.05$ ,  $F = 52.6$ ,  $df = 5$ ,  $R^2 = 0.8238$ ; DNP model vs. Control,  $P < 0.05$ , Mean Diff. =  $-4.135$ ,  $t = 11.91$ ; DNP model + H<sub>2</sub>S-L vs. Control,  $P < 0.05$ , Mean Diff. =  $-3.895$ ,

$t = 11.22$ ; DNP model + H<sub>2</sub>S-M vs. Control,  $P < 0.05$ , Mean Diff. =  $-4.065$ ,  $t = 11.71$ ; DNP model + H<sub>2</sub>S-H vs. Control,  $P < 0.05$ , Mean Diff. =  $-3.775$ ,  $t = 10.88$ ), but the three concentrations of H<sub>2</sub>S did not significantly change it compared to DNP model. The mRNA and protein levels of eNOS were not significantly changed in the DNP group, DNP model + H<sub>2</sub>S-L, DNP model + H<sub>2</sub>S-M, or DNP model + H<sub>2</sub>S-H groups compared to Control. The mRNA and protein level of nNOS were enhanced in the DNP group (mRNA:  $P < 0.05$ ,  $F = 32.41$ ,  $df = 5$ ,  $R^2 = 0.7501$ ; DNP model vs. Control,  $P < 0.05$ , Mean Diff. =  $0.038$ ,  $t = 0.2461$ ; DNP model + H<sub>2</sub>S-L vs. Control,  $P < 0.05$ , Mean Diff. =  $-0.072$ ,  $t = 0.4664$ ; DNP model + H<sub>2</sub>S-M vs. Control,  $P < 0.05$ , Mean Diff. =  $-1.102$ ,  $t = 7.138$ ; DNP model + H<sub>2</sub>S-H vs. Control,  $P < 0.05$ , Mean Diff. =  $-1.212$ ,  $t = 7.851$ . Protein level:  $P < 0.05$ ,  $F = 93.87$ ,  $df = 5$ ,  $R^2 = 0.8968$ ; DNP model vs. Control,  $P < 0.05$ , Mean Diff. =  $-0.017$ ,  $t = 0.09419$ ; DNP model + H<sub>2</sub>S-L vs. Control,  $P < 0.05$ , Mean Diff. =  $0.006$ ,  $t = 0.03324$ ; DNP model + H<sub>2</sub>S-M vs. Control,  $P < 0.05$ , Mean Diff. =  $-2.097$ ,  $t = 11.62$ ; DNP model + H<sub>2</sub>S-H vs. Control,  $P < 0.05$ , Mean Diff. =  $-2.211$ ,  $t = 12.25$ ), which were significantly inhibited by the treatment of middle and higher concentrations of H<sub>2</sub>S (mRNA: DNP model vs. DNP model + H<sub>2</sub>S-M,  $P < 0.05$ , Mean Diff. =  $-1.140$ ,  $t = 7.384$ ; DNP model vs. DNP model + H<sub>2</sub>S-H,  $P < 0.05$ , Mean Diff. =  $-1.250$ ,  $t = 8.097$ . Protein level: DNP model vs. DNP model + H<sub>2</sub>S-M,  $P < 0.05$ , Mean Diff. =  $-2.080$ ,  $t = 11.52$ ; DNP model vs. DNP model + H<sub>2</sub>S-H,  $P < 0.05$ , Mean Diff. =  $-2.194$ ,  $t = 12.16$ ).

### Inhibition of nNOS abolished the anti-nociceptive effect of H<sub>2</sub>S

To further explore the role of NOS, we treated rats with iNOS inhibitor 1400 W and nNOS inhibitor 7-NI, then measured the changes in MWT and TWL of rats. The results (Figure 4) showed that none of the three concentrations of

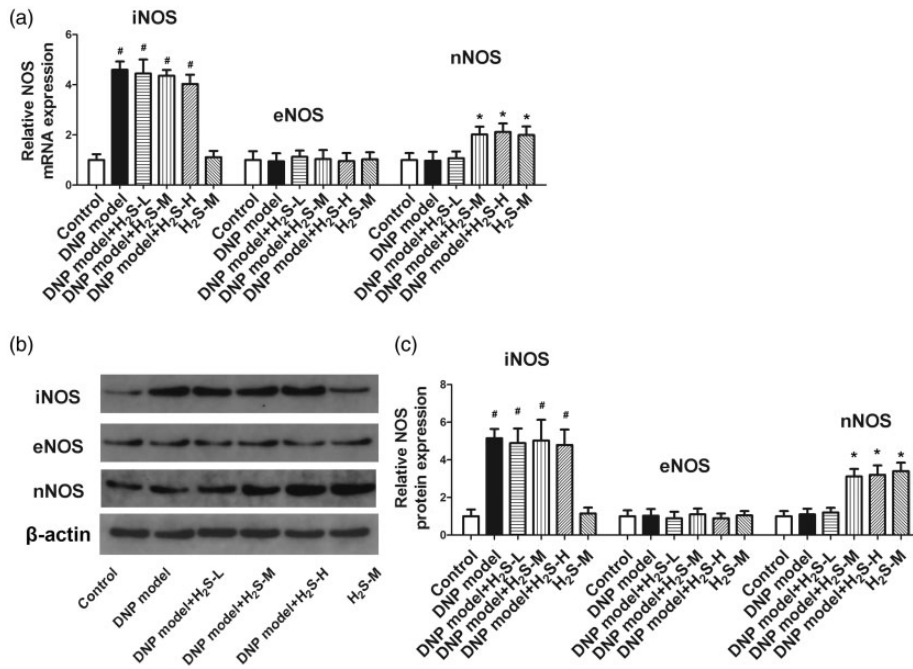


**Figure 3.** Changes in the mRNA and protein level of iNOS, nNOS, and eNOS in the spinal cord of rats. Figure 3(a) shows the changes in mRNA levels of iNOS, nNOS, and eNOS; Figure 3(b) shows the representative blots of iNOS, nNOS, and eNOS; Figure 3(c) shows the protein levels of iNOS, nNOS, and eNOS in the spinal cord. The values are expressed as Mean  $\pm$  S.E.M. The mRNA and protein level of iNOS, nNOS and eNOS in the spinal cord of rats were measured at six weeks after STZ injection. H<sub>2</sub>S-L: lower concentration of H<sub>2</sub>S (10 ppm); H<sub>2</sub>S-M: middle concentration of H<sub>2</sub>S (20 ppm); H<sub>2</sub>S-H: higher concentration of H<sub>2</sub>S (40 ppm). <sup>#</sup>*P* < 0.05 compared to Control; \**P* < 0.05 compared to DNP model. *n* = 12 per group.

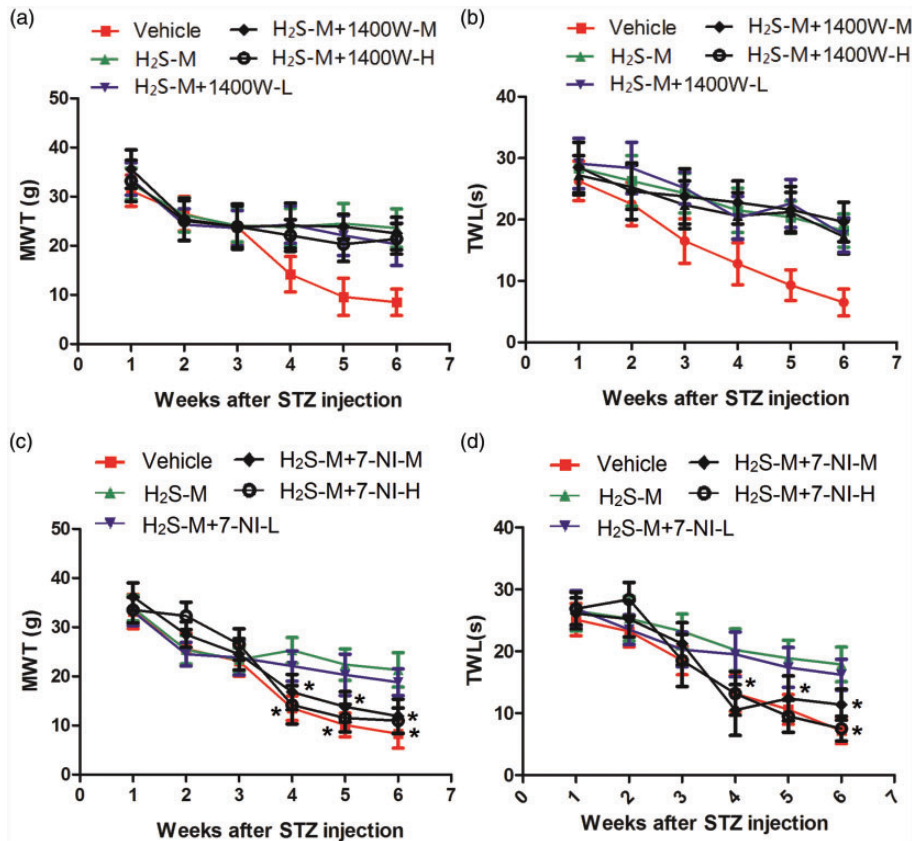


**Figure 4.** Changes in the mechanical allodynia and thermal hyperalgesia by iNOS and nNOS inhibitors. Figure 4(a) and (b) shows the changes in MWT and TWL by iNOS inhibitor 1400 W; Figure 4(c) and (d) shows the changes in MWT and TWL by nNOS inhibitor 7-NI. The values are expressed as Mean  $\pm$  S.E.M. All rats received a DNP model. The MWT and TWL of rats were measured every Monday for six weeks, beginning from one-week post-STZ injection. H<sub>2</sub>S-M: middle concentration of H<sub>2</sub>S (20 ppm); 1400 W-L: lower concentration of 1400 W (1  $\mu$ g); 1400 W-M: middle concentration of 1400 W (5  $\mu$ g); 1400 W-H: higher concentration of 1400 W (10  $\mu$ g); 7-NI-L: lower concentration of 7-NI (1  $\mu$ g); 7-NI-M: middle concentration of 7-NI (10  $\mu$ g); 7-NI-H: higher concentration of 7-NI (100  $\mu$ g). MWT: mechanical withdrawal threshold; TWL: thermal withdrawal latency. \**P* < 0.05 compared to H<sub>2</sub>S-M. *n* = 12 per group. (A color version of this figure is available in the online journal.)

1400 W significantly changed the MWT and TWL ( $P > 0.05$ ). Lower concentration of 7-NI did not significantly change the MWT and TWL, but the middle and higher concentrations of 7-NI significantly decreased the MWT and TWL compared to H<sub>2</sub>S-M group from the fourth week after STZ injection (MWT:  $P < 0.05$ ,  $F = 106.4$ ,  $df = 4$ ,  $R^2 = 0.8852$ ; H<sub>2</sub>S-M vs. H<sub>2</sub>S-M + 7-NI-M,  $P < 0.05$ , Mean Diff. = 8.583,  $t = 11.56$ ; H<sub>2</sub>S-M vs. H<sub>2</sub>S-M + 7-NI-H,  $P < 0.05$ , Mean Diff. = 11.37,  $t = 15.31$ . TWL:  $P < 0.05$ ,  $F = 71.24$ ,  $df = 4$ ,  $R^2 = 0.8382$ ; H<sub>2</sub>S-M vs. H<sub>2</sub>S-M + 7-NI-M,  $P < 0.05$ , Mean Diff. = 10.08,  $t = 13.62$ ; H<sub>2</sub>S-M vs. H<sub>2</sub>S-M + 7-NI-H,  $P < 0.05$ , Mean Diff. = 7.318,  $t = 9.889$ ).

### Inhibitors of sGC and PKG suppressed the anti-nociceptive effect of H<sub>2</sub>S

To explore the role of sGC and PKG, we treated rats with sGC inhibitor ODQ and PKG inhibitor KT5823, then measured the changes in MWT and TWL of rats. As shown in Figure 5, compared to H<sub>2</sub>S-M, the MWT and TWL were significantly decreased by all the three concentrations of ODQ (MWT:  $P < 0.05$ ,  $F = 223.0$ ,  $df = 4$ ,  $R^2 = 0.9419$ ; H<sub>2</sub>S-M vs. H<sub>2</sub>S-M + ODQ-M,  $P < 0.05$ , Mean Diff. = 8.950,  $t = 19.15$ ; H<sub>2</sub>S-M vs. H<sub>2</sub>S-M + ODQ-H,  $P < 0.05$ , Mean Diff. = 12.18,  $t = 26.07$ . TWL:  $P < 0.05$ ,  $F = 96.55$ ,  $df = 5$ ,  $R^2 = 0.8753$ ; H<sub>2</sub>S-M vs. H<sub>2</sub>S-M + ODQ-M,  $P < 0.05$ , Mean Diff. = 8.900,  $t = 18.93$ ; H<sub>2</sub>S-M vs. H<sub>2</sub>S-M + ODQ-H,  $P < 0.05$ , Mean Diff. = 6.525,  $t = 13.66$ ) and middle and higher concentrations

of KT5823 from the fourth week after STZ injection (MWT:  $P < 0.05$ ,  $F = 52.15$ ,  $R^2 = 0.7914$ ; H<sub>2</sub>S-M vs. H<sub>2</sub>S-M + ODQ-M,  $P < 0.05$ , Mean Diff. = 7.417,  $t = 10.83$ ; H<sub>2</sub>S-M vs. H<sub>2</sub>S-M + ODQ-H,  $P < 0.05$ , Mean Diff. = 7.958,  $t = 11.62$ . TWL:  $P < 0.05$ ,  $F = 60.97$ ,  $R^2 = 0.8160$ ; H<sub>2</sub>S-M vs. H<sub>2</sub>S-M + ODQ-M,  $P < 0.05$ , Mean Diff. = 8.367,  $t = 12.20$ ; H<sub>2</sub>S-M vs. H<sub>2</sub>S-M + ODQ-H,  $P < 0.05$ , Mean Diff. = 8.442,  $t = 12.31$ ). These results suggested that inhibition of sGC and PKG abolished the anti-nociceptive effect of H<sub>2</sub>S.

### H<sub>2</sub>S increased the protein expression of PKG1, which was suppressed by the inhibitors of nNOS, sGC, and PKG

To further confirm the role of PKG, we measured the mRNA and protein level of PKG1 after rats were treated with STZ, H<sub>2</sub>S or inhibitors of nNOS, sGC, and PKG. The results are shown in Figure 6. The mRNA and protein levels of PKG1 were not changed by the DNP model, but were significantly increased by middle and higher concentrations of H<sub>2</sub>S (mRNA:  $P < 0.05$ ,  $F = 1051$ ,  $df = 5$ ,  $R^2 = 0.9876$ . DNP model vs. DNP model + H<sub>2</sub>S-M,  $P < 0.05$ , Mean Diff. = -2.406,  $t = 40.40$ ; DNP model vs. DNP model + H<sub>2</sub>S-H,  $P < 0.05$ , Mean Diff. = -2.599,  $t = 43.65$ . Protein level:  $P < 0.05$ ,  $F = 581.3$ ,  $df = 5$ ,  $R^2 = 0.9778$ . DNP model vs. DNP model + H<sub>2</sub>S-M,  $P < 0.05$ , Mean Diff. = -1.529,  $t = 23.95$ ; DNP model vs. DNP model + H<sub>2</sub>S-H,  $P < 0.05$ , Mean Diff. = -2.101,

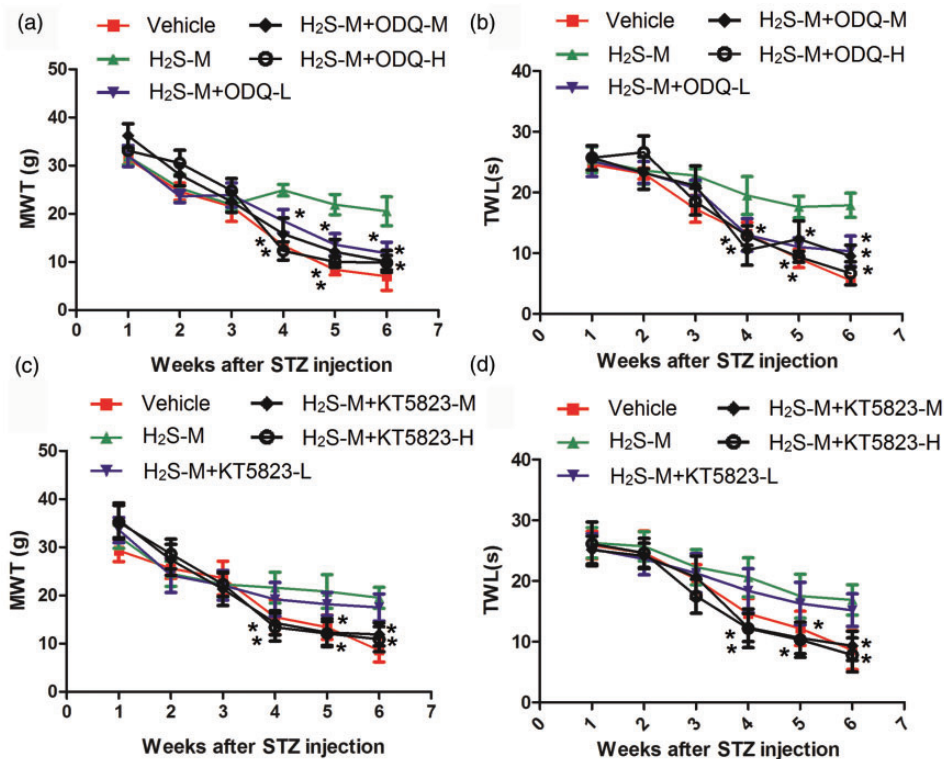


**Figure 5.** Changes in the mechanical allodynia and thermal hyperalgesia by sGC and PKG inhibitors. Figure 5(a) and (b) shows the changes in MWT and TWL by sGC inhibitor ODQ; Figure 5(c) and (d) shows the changes in MWT and TWL by PKG inhibitor KT5823. The values are expressed as Mean  $\pm$  S.E.M. All rats received a DNP model. The MWT and TWL of rats were measured every Monday for six weeks, beginning from one-week post-STZ injection. H<sub>2</sub>S-M: middle concentration of H<sub>2</sub>S (20 ppm); ODQ-L: lower concentration of ODQ (1  $\mu$ g); ODQ-M: middle concentration of ODQ (10  $\mu$ g); ODQ-H: higher concentration of ODQ (20  $\mu$ g); KT5823-L: lower concentration of KT5823 (100 ng); KT5823-M: middle concentration of KT5823 (500 ng); KT5823-H: higher concentration of KT5823 (1  $\mu$ g). MWT: mechanical withdrawal threshold; TWL: thermal withdrawal latency. \* $P < 0.05$  compared to H<sub>2</sub>S-M.  $n = 12$  per group. (A color version of this figure is available in the online journal.)

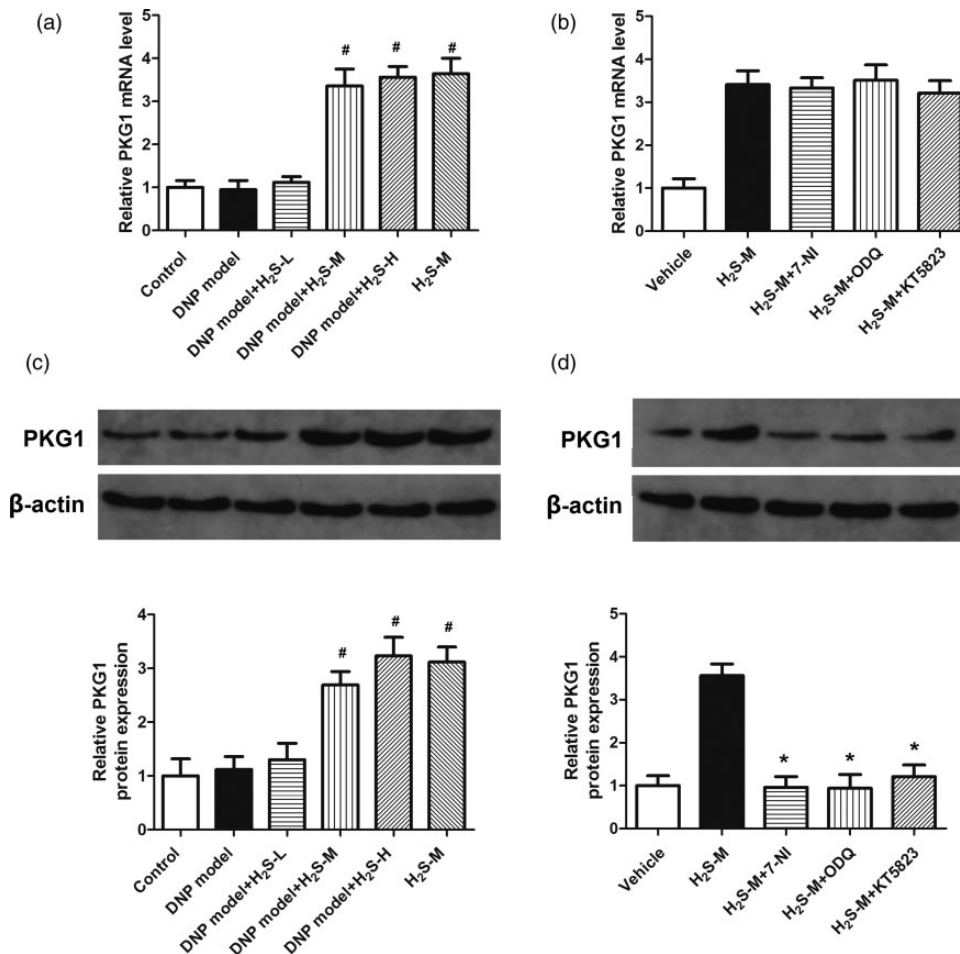


**Figure 6.** Changes in the mRNA and protein expression of PKG1 in the spinal cord by H<sub>2</sub>S and inhibitors of nNOS, sGC, and PKG. Figure 6(a) shows the changes in mRNA levels of PKG1 by H<sub>2</sub>S; Figure 6(b) shows the changes in mRNA levels of PKG1 by H<sub>2</sub>S; Figure 6(c) shows the representative blots and protein level of PKG1 after rat were treated with H<sub>2</sub>S; Figure 6(d) shows the representative blots and protein level of PKG1 after rat were treated with inhibitors of nNOS, sGC, and PKG. The values are expressed as Mean  $\pm$  S.E.M. H<sub>2</sub>S-L: lower concentration of H<sub>2</sub>S (10 ppm); H<sub>2</sub>S-M: middle concentration of H<sub>2</sub>S (20 ppm); H<sub>2</sub>S-H: higher concentration of H<sub>2</sub>S (40 ppm). H<sub>2</sub>S-M + 7-NI: 20 ppm H<sub>2</sub>S + 10  $\mu$ g 7-NI; H<sub>2</sub>S-M+ODQ: 20 ppm H<sub>2</sub>S + 10  $\mu$ g ODQ; H<sub>2</sub>S-M+KT5823: 20 ppm H<sub>2</sub>S-M + 500 ng KT5823. #*P* < 0.05 compared to DNP model; \**P* < 0.05 compared to H<sub>2</sub>S-M. *n* = 12 per group.

*t* = 32.90). Treatment of inhibitors of nNOS, sGC, and PKG (7-NI, ODQ, and KT5823) all significantly decreased the protein level of PKG1 (*P* < 0.05, *F* = 763.9, *df* = 4, *R*<sup>2</sup> = 0.9823. H<sub>2</sub>S-M vs. H<sub>2</sub>S-M + 7-NI, *P* < 0.05, Mean Diff. = -2.544, *t* = 44.38; H<sub>2</sub>S-M vs. H<sub>2</sub>S-M + ODQ, *P* < 0.05, Mean Diff. = 2.583, *t* = 45.05; H<sub>2</sub>S-M vs. H<sub>2</sub>S-M + KT5823, *P* < 0.05, Mean Diff. = 2.320, *t* = 40.47), but did not change its mRNA level.

### CTOP abolished the anti-nociceptive effect of H<sub>2</sub>S

To explore the role of opioid receptor, we treated rats with H<sub>2</sub>S and different concentrations of Nor-BNI, CTOP, and naltrindole, then measured the changes in MWT and TWL of rats. As shown in Figure 7, none of the three concentrations of Nor-BNI or naltrindole significantly changed the MWT and TWL. They were significantly decreased by all the three concentrations of CTOP from the fourth week after STZ injection compared to H<sub>2</sub>S-M group (MWT: *P* < 0.05, *F* = 75.59, *df* = 4, *R*<sup>2</sup> = 0.8461; H<sub>2</sub>S-M vs. H<sub>2</sub>S-M + CTOP-L, *P* < 0.05, Mean Diff. = 6.875, *t* = 11.45; H<sub>2</sub>S-M vs. H<sub>2</sub>S-M + CTOP-M, *P* < 0.05, Mean Diff. = 9.650,

*t* = 16.07; H<sub>2</sub>S-M vs. H<sub>2</sub>S-M + CTOP-H, *P* < 0.05, Mean Diff. = 3.108, *t* = 5.175. TWL: *P* < 0.05, *F* = 102.8, *df* = 4, *R*<sup>2</sup> = 0.8820; H<sub>2</sub>S-M vs. H<sub>2</sub>S-M + CTOP-L, *P* < 0.05, Mean Diff. = 5.825, *t* = 10.56; H<sub>2</sub>S-M vs. H<sub>2</sub>S-M + CTOP-M, *P* < 0.05, Mean Diff. = 8.367, *t* = 15.16; H<sub>2</sub>S-M vs. H<sub>2</sub>S-M + CTOP-H, *P* < 0.05, Mean Diff. = 10.33, *t* = 18.72), indicating that inhibition of  $\mu$ -opioid receptor abolished the anti-nociceptive effect of H<sub>2</sub>S.

### Discussion

Due to the poor understanding of the underlying pathogenic mechanism of DNP and the lack of effective clinical treatments, DNP has been major suffering of diabetes patients. Therefore, in-depth research on the pathogenesis of DNP may help to improve life quality. The present work established a DNP animal model and revealed that inhalation of H<sub>2</sub>S gas improved MA/TH in DNP model rats without affecting the blood glucose level and body mass. It increased the mRNA and protein level of nNOS, and the inhibitor of nNOS, 7-NI, abolished the anti-nociceptive effect of H<sub>2</sub>S. Furthermore, inhibitors of sGC and PKG



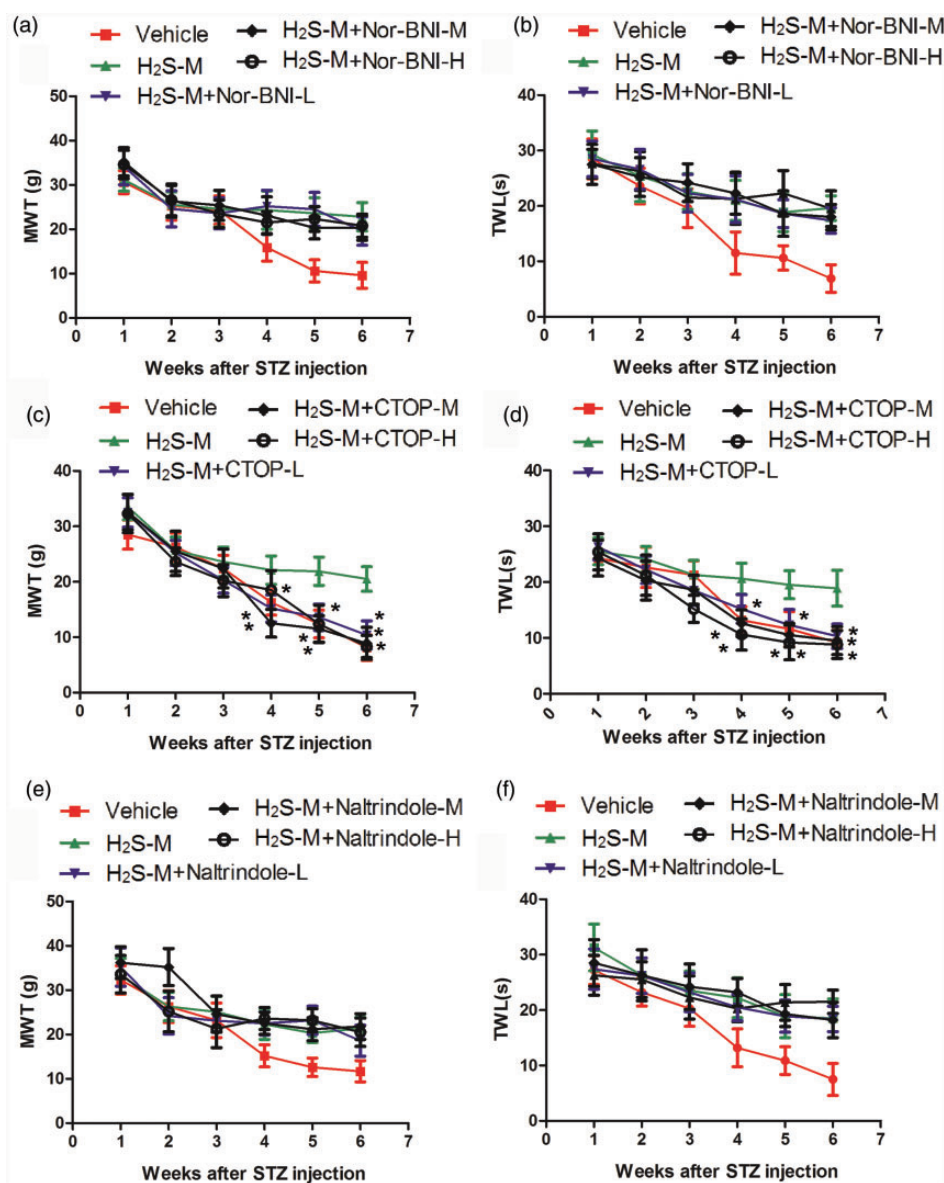


**Figure 7.** Changes in the mechanical allodynia and thermal hyperalgesia by opioid receptor antagonists. Figure 7(a) and (b) shows the changes in MWT and TWL by  $\kappa$ -opioid receptor antagonist Nor-BNI; Figure 7(c) and (d) shows the changes in MWT and TWL by  $\mu$ -opioid receptor CTOP; Figure 7(e) and (f) shows the changes in MWT and TWL by  $\delta$ -opioid receptor antagonist naltrindole. The values are expressed as Mean  $\pm$  S.E.M. The MWT and TWL of rats were measured every Monday for six weeks, beginning from one-week post-STZ injection. H<sub>2</sub>S-M: middle concentration of H<sub>2</sub>S (20 ppm); Nor-BNI-L: 10  $\mu$ g Nor-BNI; Nor-BNI-M: 20  $\mu$ g Nor-BNI-M; Nor-BNI-H: 40  $\mu$ g Nor-BNI; CTOP-L: 1  $\mu$ g CTOP-L; CTOP-M: 10  $\mu$ g CTOP; CTOP-H: 20  $\mu$ g CTOP; Naltrindole-L: 5  $\mu$ g Naltrindole; Naltrindole-M: 10  $\mu$ g Naltrindole; Naltrindole-H: 20  $\mu$ g Naltrindole. MWT: mechanical withdrawal threshold; TWL: thermal withdrawal latency. \* $P < 0.05$  compared to H<sub>2</sub>S-M.  $n = 12$  per group. (A color version of this figure is available in the online journal.)

could also abolish the anti-nociceptive effect of H<sub>2</sub>S. The expression of PKG1 was found to be increased by H<sub>2</sub>S, which was reversed by the inhibitors of nNOS, sGC, and PKG. Finally, CTOP, a  $\mu$ -opioid receptor antagonist, abolished the effect of H<sub>2</sub>S, indicating that  $\mu$ -opioid receptor participated in the anti-nociceptive action of H<sub>2</sub>S.

At present, animal models of diabetes are mostly induced by the single injection of STZ in the abdominal cavity. STZ is a powerful alkylating agent which can alkylate DNA. It makes it difficult to repair DNA, and then interferes with glucose transport and destroys islet  $\beta$  cells and induces diabetes.<sup>40</sup> The results of this experiment indicated that the DNP rat model was successfully established.

As shown in Figure 1, lower concentration of H<sub>2</sub>S did not significantly change the MWT and TWL of rats compared to Control, but middle and higher concentrations of H<sub>2</sub>S significantly increased them from the fourth week after STZ treatment compared to DNP group. The treatment of H<sub>2</sub>S, however, did not significantly affect the blood glucose level and body mass (Figure 2), indicating that the effect of H<sub>2</sub>S was not associated with the blood glucose level or the severity of STZ-induced diabetics.

The nNOS and eNOS are actively expressed in the resting state and can catalyze the production of a small amount of NO, which can relax blood vessels and regulate physiological processes such as pain.<sup>41</sup> During the formation of

neuropathic pain, activated spinal NOS can produce NO. As an important neuron messenger, NO plays an important role in signal pathways at the spinal level. Peripheral stimulation causes damage and produces adenosine triphosphate, substance P, and excitatory amino acids, which bind to glial cell receptors and lead to glial cell activation. Activated microglia expresses iNOS and produces large amounts of NO, which in turn activate astrocytes and increase the excitability of pain transmitting neurons.<sup>42–44</sup> Our result indicated that nNOS participated in the antinociception of H<sub>2</sub>S. Publications have shown that the mechanism of NOS in neuropathic pain is complicated, and the research outcomes are controversial. On one hand, it is believed that afferent neurons release glutamic acid in the spinal cord, activate N-methyl-D-aspartic acid receptors, cause Ca<sup>+</sup> influx and activate NOS. Activated NOS produce NO, which can diffuse through the cell membrane to the presynaptic membrane and promote the release of glutamic acid as well as pain sensitivity.<sup>45</sup> Some other literatures have shown that NO/cGMP activated PKG and some potassium channels, therefore caused antinociception.<sup>46</sup> Stimulation of the NO/cGMP/PKG signals may open potassium channels and produce anti-nociceptive effects.<sup>47–49</sup> NO can increase cGMP in cells by activating sGC. This present work found that H<sub>2</sub>S can reduce pain sensitivity in DNP and increase the expression of nNOS genes and proteins. The present study, by observing the effects of the inhibitors on the anti-nociceptive action of H<sub>2</sub>S, suggested that the NO/cGMP/PKG pathway participated in the action of H<sub>2</sub>S in DNP model. PKG has a variety of physiological functions<sup>50</sup> and controls a variety of physiological activities. PKG1 is mainly found in the nervous system.<sup>51</sup> PKG2 exists only in the plasma membrane and is only distributed in the kidney, cerebellum, and mucosa.<sup>52</sup> Therefore, the mRNA and protein levels of spinal cord PKG1 were measured to confirm its involvement in the action of H<sub>2</sub>S. The results indicated that H<sub>2</sub>S could activate the protein expression of PKG1, but not the mRNA levels of it to exert the anti-nociceptive effect.

Previous literatures have shown that in pain modulation, the opioid receptor is essential in the anti-nociceptive effect of many analgesic compounds. For instance, Zakaria *et al.*<sup>53</sup> found out that petroleum ether extract of *C. nutans* exerted anti-nociceptive activity by activating opioid receptors and NO/cGMP pathway. Mehanna *et al.*<sup>54</sup> investigated the anti-nociceptive effect of tadalafil in various pain models and revealed that the opioid receptors and NO/cGMP pathway were involved. The investigation of Hervera *et al.*<sup>55</sup> also suggested that  $\mu$ -opioid receptor interacted with NO/cGMP/PKG/KATP signaling pathway. We measured the MWT and TWL after rats were treated with H<sub>2</sub>S and Nor-BNI, CTOP or naltrindole. The results indicated that inhibition of the  $\mu$ -opioid receptor abolished the anti-nociceptive effects of H<sub>2</sub>S. This result suggests that the  $\mu$ -opioid receptor is involved in the antinociception of H<sub>2</sub>S.

In the end, the limitation of the present investigation has to be noted. First, this is a preliminary animal study, in which all conditions were well controlled. Whether H<sub>2</sub>S can attenuate DNP in the clinical situation still needs

inspection. Second, as H<sub>2</sub>S can regulate many signal pathways in the body, NO/cGMP/PKG pathway and the  $\mu$ -opioid receptor may not be the only mechanism of its action. More potential mechanisms and target molecules should be explored in the future.

In conclusion, the present confirmed that inhalation of H<sub>2</sub>S may attenuate the diabetic neuropathic pain through NO/cGMP/PKG pathway and the  $\mu$ -opioid receptor. It provides us the animal study foundation for the use of H<sub>2</sub>S on DNP and clarifies some target molecules in the pain modulation of DNP.

**Authors' contributions:** HL performed the animal study; SLL wrote the manuscript; ZW performed the statistical analysis; YLZ did the literature research; KGW designed and financially supported the study.

#### DECLARATION OF CONFLICTING INTERESTS

The author(s) declared no potential conflicts of interest with respect to the research, authorship, and/or publication of this article.

#### FUNDING

The author(s) received no financial support for the research, authorship, and/or publication of this article.

#### ORCID iD

Kaiguo Wang  <https://orcid.org/0000-0002-9113-0147>

#### REFERENCES

- Sharma K. Mitochondrial hormesis and diabetic complications. *Diabetes* 2015;**64**:663–72
- Hicks CW, Selvin E. Epidemiology of peripheral neuropathy and lower extremity disease in diabetes. *Curr Diab Rep* 2019;**19**:86
- Iqbal Z, Azmi S, Yadav R, Ferdousi M, Kumar M, Cuthbertson DJ, Lim J, Malik RA, Alam U. Diabetic peripheral neuropathy: epidemiology, diagnosis, and pharmacotherapy. *Clin Ther* 2018;**40**:828–49
- Morales-Vidal S, Morgan C, McCoyd M, Hornik A. Diabetic peripheral neuropathy and the management of diabetic peripheral neuropathic pain. *Postgrad Med* 2012;**124**:145–53
- Didangelos T, Doupis J, Veves A. Painful diabetic neuropathy: clinical aspects. *Handb Clin Neurol* 2014;**126**:53–61
- Singh R, Kishore L, Kaur N. Diabetic peripheral neuropathy: current perspective and future directions. *Pharmacol Res* 2014;**80**:21–35
- Bitar MS, Ayed AK, Abdel-Halim SM, Isenovic ER, Al-Mulla F. Inflammation and apoptosis in aortic tissues of aged type II diabetes: amelioration with alpha-lipoic acid through phosphatidylinositol 3-kinase/akt- dependent mechanism. *Life Sci* 2010;**86**:844–53
- Mousa SA, Shaqura M, Khalefa BI, Zöllner C, Schaad L, Schneider J, Shippenberg TS, Richter JF, Hellweg R, Shakibaei M, Schäfer M. Rab7 silencing prevents  $\mu$ -opioid receptor lysosomal targeting and rescues opioid responsiveness to strengthen diabetic neuropathic pain therapy. *Diabetes* 2013;**62**:1308–19
- Robinson CC, Barreto RPG, Plentz R. Effects of whole body vibration in individuals with diabetic peripheral neuropathy: a systematic review. *J Musculoskelet Neuronal Interact* 2018;**18**:382–8
- Sá-Caputo DC, Paineiras-Domingos LL, Oliveira R, Neves MFT, Brandão A, Marin PJ, Sañudo B, Furness T, Taiar R, Bernardo-Filho M. Acute effects of Whole-Body vibration on the pain level, flexibility, and cardiovascular responses in individuals with metabolic syndrome. *Dose Response* 2018;**16**:1559325818802139

11. Gomes-Neto M, de Sá-Caputo DDC, Paineiras-Domingos LL, Brandão AA, Neves MF, Marin PJ, Sañudo B, Bernardo-Filho M. Effects of Whole-Body vibration in older adult patients with type 2 diabetes mellitus: a systematic review and Meta-Analysis. *Can J Diab* 2019;**43**:524–9
12. Xu L, Zhang Y, Huang Y. Advances in the treatment of neuropathic pain. *Adv Exp Med Biol* 2016;**904**:117–29
13. Zhao Y, Biggs TD, Xian M. Hydrogen sulfide (H<sub>2</sub>S) releasing agents: chemistry and biological applications. *Chem Commun* 2014;**50**:11788–805
14. Yang N, Liu Y, Li T, Tuo Q. Role of hydrogen sulfide in chronic diseases. *DNA Cell Biol* 2020;**39**:187–96
15. Ishigami M, Hiraki K, Umemura K, Ogasawara Y, Ishii K, Kimura H. A source of hydrogen sulfide and a mechanism of its release in the brain. *Antioxid Redox Signal* 2009;**11**:205–14
16. Kawabata A, Ishiki T, Nagasawa K, Yoshida S, Maeda Y, Takahashi T, Sekiguchi F, Wada T, Ichida S, Nishikawa H. Hydrogen sulfide as a novel nociceptive messenger. *Pain* 2007;**132**:74–81
17. Lee AT, Shah JJ, Li L, Cheng Y, Moore PK, Khanna S. A nociceptive-intensity-dependent role for hydrogen sulphide in the formalin model of persistent inflammatory pain. *Neuroscience* 2008;**152**:89–96
18. Maeda Y, Aoki Y, Sekiguchi F, Matsunami M, Takahashi T, Nishikawa H, Kawabata A. Hyperalgesia induced by spinal and peripheral hydrogen sulfide: evidence for involvement of Cav3.2 T-type calcium channels. *Pain* 2009;**142**:127–32
19. Cunha TM, Dal-Secco D, Verri WA, Jr., Guerrero AT, Souza GR, Vieira SM, Lotufo CM, Neto AF, Ferreira SH, Cunha FQ. Dual role of hydrogen sulfide in mechanical inflammatory hypernociception. *Eur J Pharmacol* 2008;**590**:127–35
20. Distrutti E, Sediari L, Mencarelli A, Renga B, Orlandi S, Antonelli E, Roviezzo F, Morelli A, Cirino G, Wallace JL, Fiorucci S. Evidence that hydrogen sulfide exerts antinociceptive effects in the gastrointestinal tract by activating KATP channels. *J Pharmacol Exp Ther* 2006;**316**:325–35
21. Chen H, Xie K, Chen Y, Wang Y, Lian N, Zhang K, Yu Y. Nrf2/HO-1 signaling pathway participated in the protection of hydrogen sulfide on neuropathic pain in rats. *Int Immunopharmacol* 2019;**75**:105746
22. Zhuang L, Li K, Wang G, Shou T, Gao C, Mao Y, Bao M, Zhao M. Preconditioning with hydrogen sulfide prevents bone cancer pain in rats through a proliferator-activated receptor gamma/p38/jun N-terminal kinase pathway. *Exp Biol Med* 2018;**243**:57–65
23. Tang G, Wu L, Liang W, Wang R. Direct stimulation of K(ATP) channels by exogenous and endogenous hydrogen sulfide in vascular smooth muscle cells. *Mol Pharmacol* 2005;**68**:1757–64
24. Streng T, Axelsson HE, Hedlund P, Andersson DA, Jordt SE, Bevan S, Andersson KE, Hogestatt ED, Zygmunt PM. Distribution and function of the hydrogen sulfide-sensitive TRPA1 ion channel in rat urinary bladder. *Eur Urol* 2008;**53**:391–9
25. Kubo S, Kurokawa Y, Doe I, Masuko T, Sekiguchi F, Kawabata A. Hydrogen sulfide inhibits activity of three isoforms of recombinant nitric oxide synthase. *Toxicology* 2007;**241**:92–7
26. Han J, Kim N, Joo H, Kim E, Earm YE. ATP-sensitive K(+) channel activation by nitric oxide and protein kinase G in rabbit ventricular myocytes. *Am J Physiol Heart Circ Physiol* 2002;**283**:1545–54
27. Levy D, Strassman AM. Modulation of dural nociceptor mechanosensitivity by the nitric oxide-cyclic GMP signaling cascade. *J Neurophysiol* 2004;**92**:766–72
28. Kalyanaraman H, Schwaerzer G, Ramdani G, Castillo F, Scott BT, Dillmann W, Sah RL, Casteel DE, Pilz RB. Protein kinase G activation reverses oxidative stress and restores osteoblast function and bone formation in male mice with type 1 diabetes. *Diabetes* 2018;**67**:607–23
29. Chen SR, Pan HL. Spinal nitric oxide contributes to the analgesic effect of intrathecal [d-pen<sub>2</sub>,d-pen<sub>5</sub>]-enkephalin in normal and diabetic rats. *Anesthesiology* 2003;**98**:217–22
30. Chen SR, Eisenach JC, Pan HL. Intrathecal S-nitroso-N-acetylpenicillamine and L-cysteine attenuate nerve injury-induced allodynia through noradrenergic activation in rats. *Neuroscience* 2000;**101**:759–65
31. Mixcoatl-Zecuatl T, Flores-Murrieta FJ, Granados-Soto V. The nitric oxide-cyclic GMP-protein kinase G-K+ channel pathway participates in the antiallodynic effect of spinal gabapentin. *Eur J Pharmacol* 2006;**531**:87–95
32. Ge H, Guan S, Shen Y, Sun M, Hao Y, He L, Liu L, Yin C, Huang R, Xiong W, Gao Y. Dihydromyricetin affects BDNF levels in the nervous system in rats with comorbid diabetic neuropathic pain and depression. *Sci Rep* 2019;**9**:019–51124
33. Sun Q, Wang C, Yan B, Shi X, Shi Y, Qu L, Liang X. Jinmaitong ameliorates diabetic peripheral neuropathy through suppressing TXNIP/NLRP3 inflammasome activation in the Streptozotocin-Induced diabetic rat model. *Diabetes Metab Syndr* 2019;**12**:2145–55
34. Kida K, Yamada M, Tokuda K, Marutani E, Kakinohana M, Kaneki M, Ichinose F. Inhaled hydrogen sulfide prevents neurodegeneration and movement disorder in a mouse model of Parkinson's disease. *Antioxid Redox Signal* 2011;**15**:343–52
35. Novochinskii II, Song C, Ma X, Liu X, Shore L, Lampert J, Farrauto RJ. Low-Temperature H<sub>2</sub>S removal from steam-containing gas mixtures with ZnO for fuel cell application. 1. ZnO particles and extrudates. *Energy Fuels* 2004;**18**:576–83
36. Chen T, Li H, Yin Y, Zhang Y, Liu Z, Liu H. Interactions of Notch1 and TLR4 signaling pathways in DRG neurons of in vivo and in vitro models of diabetic neuropathy. *Sci Rep* 2017;**7**:14923
37. Gibbons CR, Liu S, Zhang Y, Sayre CL, Levitch B, Moehlmann S, Shirachi DY, Quock RM. Involvement of brain opioid receptors in the anti-allodynic effect of hyperbaric oxygen in rats with sciatic nerve crush-induced neuropathic pain. *Brain Res* 2013;**1537**:111–6
38. Lui PW, Lee CH. Preemptive effects of intrathecal cyclooxygenase inhibitor or nitric oxide synthase inhibitor on thermal hypersensitivity following peripheral nerve injury. *Life Sci* 2004;**75**:2527–38
39. Zhang H, Pakeerappa P, Lee HJ, Fisher SA. Induction of PDE5 and desensitization to endogenous NO signaling in a systemic resistance artery under altered blood flow. *J Mol Cell Cardiol* 2009;**47**:57–65
40. Wang Y, Liu C, Guo QL, Yan JQ, Zhu XY, Huang CS, Zou WY. Intrathecal 5-azacytidine inhibits global DNA methylation and methyl-CpG-binding protein 2 expression and alleviates neuropathic pain in rats following chronic constriction injury. *Brain Res* 2011;**18**:64–9
41. Wang Y, Golledge J. Neuronal nitric oxide synthase and sympathetic nerve activity in neurovascular and metabolic systems. *Curr Neurovasc Res* 2013;**10**:81–9
42. Choi JI, Kim WM, Lee HG, Kim YO, Yoon MH. Role of neuronal nitric oxide synthase in the antiallodynic effects of intrathecal EGCG in a neuropathic pain rat model. *Neurosci Lett* 2012;**510**:53–7
43. Kuboyama K, Tsuda M, Tsutsui M, Toyohara Y, Tozaki-Saitoh H, Shimokawa H, Yanagihara N, Inoue K. Reduced spinal microglial activation and neuropathic pain after nerve injury in mice lacking all three nitric oxide synthases. *Mol Pain* 2011;**7**:1744–8069
44. Mor D, Bembrick AL, Austin PJ, Keay KA. Evidence for cellular injury in the midbrain of rats following chronic constriction injury of the sciatic nerve. *J Chem Neuroanat* 2011;**41**:158–69
45. Kawamata T, Omote K. Activation of spinal N-methyl-D-aspartate receptors stimulates a nitric oxide/cyclic guanosine 3,5-monophosphate/glutamate release Cascade in nociceptive signaling. *Anesthesiology* 1999;**91**:1415–24
46. Tanabe M, Nagatani Y, Saitoh K, Takasu K, Ono H. Pharmacological assessments of nitric oxide synthase isoforms and downstream diversity of NO signaling in the maintenance of thermal and mechanical hypersensitivity after peripheral nerve injury in mice. *Neuropharmacology* 2009;**56**:702–8
47. Pollema-Mays SL, Centeno MV, Ashford CJ, Apkarian AV, Martina M. Expression of background potassium channels in rat DRG is cell-specific and down-regulated in a neuropathic pain model. *Mol Cell Neurosci* 2013;**57**:1–9
48. Busserolles J, Tsantoulas C, Eschalier A, Lopez Garcia JA. Potassium channels in neuropathic pain: advances, challenges, and emerging ideas. *Pain* 2016;**157**:S7–14
49. Fan L, Guan X, Wang W, Zhao JY, Zhang H, Tiwari V, Hoffman PN, Li M, Tao YX. Impaired neuropathic pain and preserved acute pain in rats overexpressing voltage-gated potassium channel subunit Kv1.2 in primary afferent neurons. *Mol Pain* 2014;**10**:1744–8069
50. Quock LP, Zhang Y, Chung E, Ohgami Y, Shirachi DY, Quock RM. The acute antinociceptive effect of HBO(2) is mediated by a NO-cyclic GMP-PKG-KATP channel pathway in mice. *Brain Res* 2011;**12**:102–7

51. Geiselhoringer A, Gaisa M, Hofmann F, Schlossmann J. Distribution of IRAG and cGKI-isoforms in murine tissues. *FEBS Lett* 2004;**575**:19–22
52. Jarchau T, Hausler C, Markert T, Pohler D, Vanderkerckhove J, De Jonge HR, Lohmann SM, Walter U. Cloning, expression, and in situ localization of rat intestinal cGMP-dependent protein kinase II. *Proc Natl Acad Sci U S A* 1994;**91**:9426–30
53. Zakaria ZA, Abdul Rahim MH, Mohd Sani MH, Omar MH, Ching SM, Abdul Kadir A, Ahmed QU. Antinociceptive activity of petroleum ether fraction obtained from methanolic extract of *Clinacanthus nutans* leaves involves the activation of opioid receptors and NO-mediated/cGMP-independent pathway. *BMC Complement Altern Med* 2019;**19**:79
54. Mehanna MM, Domiati S, Nakkash Chmaisse H, El Mallah A. Antinociceptive effect of tadalafil in various pain models: involvement of opioid receptors and nitric oxide cyclic GMP pathway. *Toxicol Appl Pharmacol* 2018;**352**:170–5
55. Hervera A, Negrete R, Leanez S, Martin-Campos JM, Pol O. Peripheral effects of morphine and expression of mu-opioid receptors in the dorsal root ganglia during neuropathic pain: nitric oxide signaling. *Mol Pain* 2011;**7**:25

(Received December 28, 2019, Accepted March 14, 2020)